Characterizing seismites with anisotropy of magnetic susceptibility

Levi, T.[1], Weinberger, R.[1, 2], Alsop, G.I.[3] and Marco, S.[4]

1) Geological survey of Israel, Jerusalem, Israel.

2) Department of Geological and Environmental Sciences, Ben Gurion University of the Negev, Beer Sheva, Israel.

3) Department of Geology and Petroleum Geology, School of Geosciences, University of Aberdeen, Aberdeen, UK.

4) Department of Geophysics, School of Geosciences, Tel Aviv University, Israel.

ABSTRACT

Characterizing seismites is a key factor in understanding earthquake kinematics, dynamics and resulting hazards. Despite the importance of this characterization, the rearrangement of the deformed volume is typically not well understood, hampering the possibility of infering ther kinematics and dynamics of seismites. In order to overcome these difficulties, we analyzed the anisotropy of magnetic susceptibility (AMS) of various seismite types of known origin that have formed during paleoseismic activity along the Dead Sea Fault (DSF) system. In this study, the magnetic lineation (*L)* and the shape of the AMS ellipsoid (*T*) of the seismites are presented in a novel *T* versus *L* plot. Depending on the type of material, the seismites are distinguished according to the following characteristics. Injection structures are characterized by a nonlinear correlation curve; co-seismic fault-related damage zones lie on a common linear correlation curve; earthquake-triggered folds also show a linear correlation with those that have undergone major deformation and have low T and high L values. Breccia layers display a range of T and L values similar to that of primary sedimentary layers, implying that such seismites were formed by material deposited immediately after an earthquake. This novel application of AMS provides an effective tool for resolving the kinematics and dynamics of a wide variety of seismites in soft-rocks. We outline a robust procedure to infer the seismite mechanism which is helpful in recovering paleoseismic records in complex settings and defining potentially hazardous geological areas.

INTRODUCTION

Earthquake-related seismites such as deformed sediments near co-seismic faults, folds, injection structures, breccia layers and fissures are important palaeoseismic indicators that promote the understanding of many aspects of tectonics. However, it is not always possible to identify seismites and often difficult to determine their mechanism of formation through direct field observations, in particular, where rocks are massive and do not exhibit distinct markers. In this work we examine the possibility of detecting different seismite types through the analysis of Anisotropy of Magnetic Susceptibility (AMS). The AMS analysis is generally used for characterizing petrofabrics in order to reveal flow directions and for quantifying weak inelastic deformation (e.g., Schwehr and Tauxe, 2003; Borradaile and Jackson, 2004). The AMS fabric is commonly represented as an ellipsoid, whose principal axes (eigenvectors), the maximum K_1, intermediate K_2, and minimum K_3 magnetic susceptibility, correspond to k_1, k_2, and k_3 eigenvalues of the AMS. Since the AMS analysis is one of the best techniques for identifying inelastic strain preserved in rocks (e.g., Borradaile and Jackson, 2004), it can also be applied to identify and characterize deformation in seismites (e.g. Levi et al., 2006). However, attempts to correlate seismites with different processes based solely on projecting the AMS axes might lead to incorrect interpretations, because in some cases, the AMS axes of different deformation mechanisms can show a similar orientation and degree of clustering. On the other hand, the AMS parameters that represent the magnitude and the shape of the AMS ellipsoid may be useful in identifying different seismites. For example, it is well known that the magnetic lineations, $L = k_1/k_2$, begin to develop during progressive deformation, preserving the inelastic strain stored in the rocks (e.g., Parés and Pluijm, 2002) and the shape of the AMS (Jelinek, 1981), $T = (2lnk_2 - lnk_1 - lnk_3)/(lnk_1 - lnk_3)$ can be correlated with the strain magnitude and its history of deformation (e.g., Parés and Pluijm, 2003). Magnetic lineation, foliation and the shape of the AMS may reflect magnetic fabrics forming differently as a result of the deposition, transport, and deformation of rocks (Borradaile and Jackson, 2004). AMS has also been correlated with strain in rocks and the tectonic deformation of sediments (Levi and Weinberger, 2011), and has been used to characterize soft-rock deformation (Schwehr and Tauxe, 2003; Weinberger et al., 2017).

Despite the importance of characterizing seismites, no previous attempt has apparently been made to examine whether different seismites can be separated and characterized by the AMS parameters. We therefore aim to relate seismites to characteristic processes by analyzing the AMS parameters of a range of recent (<40 kyr), seismite types that formed in association with paleoseismic activity along the Dead Sea Fault (DSF) system (Fig. 1). In this study, we pursue the idea that various seismite types in soft-rocks can be detected through the use of *L* and *T* parameters.

GEOLOGIC SETTING

The DSF system (Fig. 1) is one of the most active tectonic features in the Middle East (e.g., Garfunkel et al., 2014 and references therein). It has been active since the Early Miocene (Nuriel et al., 2017 and references therein), and comprises several tectonic depressions, the most prominent of which is the Dead Sea Basin (DSB) (Fig. 1; Garfunkel et al., 2014 and references therein). The Lisan Formation was deposited in the DSB between 70 and 15 ka (Haase-Schramm et al., 2004) and exposes numerous seismities that are the focus of the present study (Fig. 1a). The lacustrine sediments of the Lisan Formation comprise a ~40 m sequence of alternating white authigenic aragonite and fine dark detrital laminae.

Paleoseismic records reveal numerous M > 5.5-6 earthquake events, as well as several M > 7 earthquake events during the late Pleistocene and the Holocene (Marco and Klinger, 2014 and references therein). During this seismic activity, different types of seismites were formed (Fig. 2): (1) a set of syn-depositional normal faults and an envelope of deformed rock volume, known as a damage zone (Levi et a., 2014); (2) folds and fold-thrust systems, which formed mass transport deposits (MTDs) at the near surface that were controlled by gravity-driven movement toward the depocenter (Alsop et al., 2012, 2017; Weinberger et al., 2017); (3) injection clastic dikes, which formed due to fluidization of the Lisan source layers during seismic events (Levi et al., 2006); (4) sheared clastic dikes, which are associated with coseismic horizontal bedding-plane slip and gouge formation (Weinberger et al., 2016) and (5) Breccia layers, which formed on the bottom of the lake by the mixing of laminated fragments in the Dead Sea water during earthquake shaking (Marco and Agnon, 2005). Following significant drying of Lake Lisan at 14-11 kyr and the occurrence of strong earthquakes, sets of clastic dykes were formed dynamically by host-rock fracturing and injection of the fluidized detrital material from the source layers (Levi et al., 2006). The injection of this fluidized material ~18 m below the surface was mainly vertical in association with turbulent flow condition, while close to the surface, the injection was horizontal and laminar (Levi et al., 2006).

THE *T-L* PLOT

AMS may be represented by a magnitude ellipsoid, where the most frequently used anisotropy parameters are the mean susceptibility k_m, the corrected anisotropy degree P ($P=k_1/k_3$), the magnetic lineation L, the magnetic foliation F and the AMS shape parameter T, measuring the range from prolate ($-1<T<0$) through neutral ($T=0$) to oblate ($0<T<1$) ellipsoids (Jelinek, 1981; Borradaile and Jackson, 2004 and references therein).

During deformation of soft-rocks, the strain ellipsoid of the strain may vary and be accompanied by formation of a lineation. Respectively, this process can be expressed as an increase in the values of L and a change in the value of T. However, the use of such plots, or similar, has not yet been implemented (but see *T-F* relations in Hrouda and Ježek eq. 12, 2014), especially in the study of soft-rock deformation.

Mathematically, the magnetic lineation L is described as:

$$L = P\,(k_3/k_2) \qquad (1)$$

Where

$$P = k_1/k_3 \qquad (2)$$

is the anisotropy degree.

The AMS shape parameter T (Jelinek, 1981) is described as:

$$T = (2lnk_2 - lnk_1 - lnk_3)/(lnk_1 - lnk_3) \qquad (3)$$

For convenience, equation (1) can be presented according to the log rules

$$ln(L) = ln\left(\frac{k_1}{k_3}\right) + ln\left(\frac{k_3}{k_2}\right) \quad (4)$$

Inserting equation (4) into equation (3), the T-L can be then described as:

$$T = \left[-\frac{2}{\ln\left(\frac{k_1}{k_3}\right)} ln(L)\right] + 1 \quad (5)$$

where $-\frac{2}{\ln\left(\frac{k_1}{k_3}\right)}$ is the slope of equation (4) and the intersection point is at T=1.

For convenience, $ln(L)$ can be approximated as L-1 (within 5% for values ranging between 1 and about 1.1) or the L values can be presented on a logarithmic axis.

In cases where the samples share similar $\frac{k_1}{k_3}$, the slope of equation (4) is expected to be constant and the correlation between T and L is linear (up to L≈2) (Fig. 3; A curve). In cases where the samples do not share similar $\frac{k_1}{k_3}$, the correlation between T and L is expected to be non-linear (Fig. 3; B curve).

On the basis of the underlying significance of the AMS parameters described above, we hypothesize that different types of seismites are diagnosed differently in the T-L plot.

MAGNETIC FABRICS OF THE LISAN SEISMITES

The white aragonite of the Lisan Formation consists mainly of diamagnetic aragonite while the dark detritus layers have positive bulk AMS susceptibility. Titanomagnetite, magnetite, and greigite are the ferromagnetic carriers in the detrital laminae (e.g., Ron et al., 2006; Levi et al., 2006, 2014).

We analyzed 588 samples of different seismite types, located in sites that are spread along ~80 km of one of the main segments of the DSB (Fig. 1a; Almog, Massada Plain, Ami'az Plain and Wadi Zin sites; DR1). Two outcrops consisting of undisturbed beds act as reference layers, and are made of alternating white aragonite and dark detritus from the Ami'az Plain (Fig. 1b). In order to test the effect of strain along the folded layers, and the effect of the material properties on the AMS parameters, the T and L values are presented in two T-L plots: (1) seismites formed of alternating aragonite-detritus laminae; and (2) seismites formed solely of detritus. Detailed AMS analysis was carried out along the folded layers.

RESULTS

Figure 4a shows the T-L plot (i.e., ln (L) values are displayed along x axis) of seismites composed of aragonite layers. The correlation obtained in this plot was linear and relatively high. Based on the seismite types, three main groups were obtained along the same correlation curve: Group (A), ranges from T=0.61 up to T=0.98 and L=1 up to L=1.002, includes the reference layer, breccia layers and sedimentary layers near the faults; Group (B) ranges from T=-0.41 up to T=0.79 and L=1.004 up to L=1.023, includes damage zones and gouges, and Group (C) ranges from T=-0.41 up to T=0.79 and L=1.004 up to L=1.023, includes folds. Detailed analysis of the folds shows that the values of L and T are arranged along the correlation curve, depending on the structural domains within the fold itself (DR2, DR3).

The T-L plot of folded layers and clastic dikes formed of injected detritus (Fig. 4b) shows that the correlation obtained for the folds (Group D) is linear and relatively high, whereas that obtained for the vertical and horizontal injections (Group E) are nonlinear and relatively low and high, respectively. The folded detrital layers are similar to the aragonite layers, in that their horizontal layers have high *T* and low *L* values. On the other hand, vertical layers in the forelimbs have low *T* and high *L* values (DR2, DR3). In clastic dikes where the material was injected horizontally, the values of *T* are high and the values of *L* are low, whereas in vertical and turbulent injections the values of *T* are low and the values of *L* are intermediate to high.

DISCUSSION AND CONCLUISIONS

During an earthquake, the evolved deformation in a rock can differ from place to place and from time to time, depending on the local geological conditions and the material properties (e.g., McCalpin, 1996; Marco and Agnon, 2005; Alsop et al., 2012, 2017; Levi et al., 2006, 2008; Weinberger et al., 2016, 2017). In order to relate magnetic fabrics of sedimentary rocks with different deformation processes, several plots of AMS parameters have been used so far, including the bootstrapped eigenvalue histogram (Tauxe, 1998; Schwehr and Tauxe, 2003); *L-F* (Parés and Pluijm, 2002, 2003;) *P*- k_m (e.g., Ferré el al., 2014) *T-P* (e.g., Cifelli et al., 2009; Aubourg, et al., 2014). It is noteworthy that none of the above mentioned plots have been tested for a large variety of seismites concurrently (DR4).

The present study shows that the common bi-parametric plots noted above fail to distinguish between seismites that have formed along progressive processes.

However, the present results show that the *T-L* plot, allows seismites of different origins to be correlated with specific types of deformation, while the type of material has a significant effect on the evolved *T* and *L* that accompanies the deformation.

Accordingly, the T-L plot shows that seismite types are organized into five main groups.

Group A (Fig. 4a,), including sedimentary layers near a fault and breccia layers, is characterized by high T and low L values. The values T and L (site average) of the breccia layers reflects the suspension and the re-deposition processes that occurred during earthquake events over the lake floor. The 'sedimentary' T and L values characterizing these layers, is evidence of these processes (Fig. 4a, and DR5). In some cases, the flow above the hangingwall was to the west (Fig 2, DR5; MS1 and MS2 outcrops), opposite to the direction of the regional transport, that is expected to move eastward toward the depocenter of the basin (Alsop and Marco, 2012; Weinberger et al., 2017). It is reasonable to assume that those processes could have lasted hours or even several days after the event.

Group B (Fig. 4A), including the damage zones, gouges (polygon #B) and Group C of folds (polygon #C), are characterized by a linear trend extending to low T and high L values. During the faulting, the damage zones and the gouges were associated with an inelastic deformation (Levi et al., 2014). This deformation is expressed by the formation of a magnetic lineation and a decrease in oblateness, as identified by the negative linear correlation curve reaching to L = 1.014 and T = 0.3 (Fig. 4a). It was previously demonstrated that the formation of this magnetic fabric did not take more than a few seconds (Levi et al., 2014). Folds are made of similar materials as the damage zones, and, hence, are expected to lie on the same linear T-L correlation curve, with constant $P = \frac{k_1}{k_3}$ (Fig. 3). However, the strain magnitude of the folds, indicating a significant shortening is likely to be higher than that of the damage zones. Therefore, in the T-L plot, the folds have high L values (up to 1.023) and low T values (up to -0.4). L and T values of several structural domains of the folds (i.e., forelimbs, hinges) are located at the extreme end of the T-L curve (Fig.4a, DR6). This indicates that the deformation along the folded layers is heterogeneous (e.g., Weinberger et al., 2017).

Group D includes folded detritus layers and injection clastic dikes (Group E) infilled by detrital material (Fig. 4b). Figure 4b shows that the $\frac{k_1}{k_3}$ of folds formed of detritus layers is linear and smaller than that of the aragonite layers. The original P of the aragonite reference layer is higher (1.028) than that of the detrital reference layer (1.016). This anisotropy difference may be related to the crystallographic structure of the aragonite needles, whose alignment causes a high anisotropy (Hrouda, 2004) compared to that of the clay and ferromagnetic minerals of the detrital layers. This difference may also be sustained during the fracturing and folding, which is confirmed by the T-L plot, showing that the greater the $\frac{k_1}{k_3}$, the lower the slope (absolute value) of a given material (Fig. 4a).

Unlike other seismite types, during the injection process, the particles completely lose their cohesion and mobilize away from the source layer; and since the shear rate may change from place to place, the sites no longer share a common $\frac{k_1}{k_3}$. Under these conditions the oblate shape of the magnetic fabric decreases (Levi et al., 2006), and the lineation is relatively low. Respectively, Figure 4b shows that the range of L and T values of the clastic dikes is almost fully distinguishable from the range of values of the folds, although both types of seismites are formed of the same detrital material. It is very likely that the variations between the flow types (Fig. 4b) are related to the differences between turbulent (high flow) and laminar flow (slow flow) conditions (Levi et al, 2006 and references therein).

There are a number of indications that can be used by applying the new T-L plot to identify the type of seismites in soft rocks (i.e., breccia layers, damage zones, folds and fluidized layers). Since the type of material has a significant effect on the initial values and evolution of *T* and *L* parameters, the data should first be displayed in accordance with the type of material (Figs. 4a, 4b). In cases where the correlation curve is nonlinear, then the seismite can be attributed to fluidization. Conversely, if the correlation curve is linear, then the seismite can be attributed to folding, development of a fault-related damage zone and deposition. Further, if the sites have low *T* and high *L* values (Figs. 4.a,b groups C and D) then the seismites can be attributed to folding accompanied by high strain. In cases where the sites are located near faults and have a range of *T-L* values similar to that of Group B (Fig. 4a), then the tested layers may be related to the development of damage zones. If the tested layers are located close to the fault and have a range of *T-L* values similar to that of Group A (Fig. 4a), it can be assumed that these layers did not undergo significant deformation. In cases where the seismites are breccia layers and have a range of *T-L* values similar to that of Group A, it can be assumed that these layers did not undergo any kind of deformation other than re-deposition. The re-deposition occurred at the surface immediately after the earthquakes, and is different from damage zones that were developed near co-seismic faults and can help to estimate the total displacement along the co-seismic fault. In cases where the range of *T-L* values differs from that of Group A and others, it can be assumed that additional processes occurred during or after the seismite formation.

This study shows that a *T-L* plot can distinguish between the kinematics by which different seismites were formed in soft-rocks. It may therefore prove helpful in recovering paleoseismic records in complex geological settings and in studying deformation such as folding and fault-related damage zones in other tectonic environments

REFERENCES

Alsop, G.I., and Marco, S. 2012, A large-scale radial pattern of seismogenic slumping towards the Dead Sea Basin: Journal of the Geological Society, v. 169, p. 99-110.

Alsop, G. I., Marco, S. Levi, T. and Weinberger R., 2017, Fold and thrust systems in Mass Transport Deposits: Journal of Structural Geology, v. 94, p. 98–115.

Borradaile, G.J., and Jackson, M., 2004, Anisotropy of magnetic susceptibility (AMS): magnetic petrofabrics of deformed rocks. In: Martín-Hernández, F., Lüneburg, C.M,. Aubourg, C., Jackson, M. (Eds.), Magnetic Fabric: Methods and Applications.: Special Publication, 238. Geological Society, London, pp. 299–360.

Cifelli, F., Mattei, M., Chadima, M., Lenser, S., and Hirt, A.M., 2009, The magnetic fabric in “undeformed clays”: AMS and neutron texture analyses from the Rif Chain (Morocco): Tectonophysics, v. 466, p. 79–88.

Ferré E.C., Gébelin, A., Till, J.L., Sassier, C. and Burmeister, K.C., 2014, Deformation and magnetic fabrics in ductile shear zones: a review: Tectonophysics, v. 629, p. 179–188.

Garfunkel, Z, Ben-Avraham, Z, and Kagan, E (Eds.)., 2014, Dead Sea Transform Fault System: Reviews, Springer, Dordrecht (2014). 359 pp.

Haase-Schramm, A., Goldstein, S.L., and Stein, M., 2004, U-Th dating of Lake Lisan aragonite (late Pleistocene Dead Sea) and implications for glacial East Mediterranean climate change: Geochimica et Cosmochimica Acta, v. 68, p. 985-1005.

Hrouda, F., 2004, Problems in interpreting AMS parameters in diamagnetic rocks: Geological Society, London, Special Publications 2004, v. 238, p. 49–59.

Hrouda, F., and Ježek, J, Frequency-dependent AMS of rocks: A tool for the investigation of the fabric of ultrafine magnetic particles: Tectonophysics, 629, p. 27-38.Jelinek, V., 1981, Characterization of magnetic fabric of rocks: Tectonophysics, 79, p. 63-67.

Levi, T., Weinberger, R., Aïfa, T., Eyal, Y., and Marco, S., 2006, Injection mechanism of clay-rich sediments into dikes during earthquakes: Geochemistry, Geophysics, Geosystems, v. 7(12). doi: 10.1029/2006GC001410.

Levi, T., Weinberger, R., Eyal, Y., Lyakhovsky, V. and Hefez, E., 2008, Velocities and driving pressures of clay-rich sediments injected into clastic dikes during earthquakes: Geophysical Journal International, v. 175, p. 1095–1107.

Levi, T., and Weinberger, R., 2011, Magnetic fabrics of diamagnetic rocks and the strain field associated with the Dead Sea fault, northern Israel: Journal of Structural Geology, v. 33, p. 566–578.

Levi, T., Weinberger, R. and Marco, S., 2014, Magnetic fabrics induced by dynamic faulting reveal damage zone sizes in soft rocks, Dead Sea basin: Geophysical Journal International, v. 199(2), p. 1214-1229.

Marco, S., and Agnon.A., 2005, High-resolution stratigraphy reveals repeated earthquake faulting in the Masada Fault Zone, Dead Sea Transform: Tectonophysics, v. 408, p. 101– 112.

Marco, S., and Klinger Y, 2014, Review of On-Fault Palaeoseismic Studies Along the Dead Sea Fault. In: Z. Garfunkel et al. (eds.), Dead Sea Transform Fault System: Reviews, Modern Approaches in Solid Earth Sciences 6, Springer Science+Business Media Dordrecht. Chapter 7: 183-205

McCalpin, J.P. (ed), 1996, Paleoseismology. International Geophysical Series, 62. Academic Press, San Diego, 588 p.

Nuriel, P., Weinberger, R., Kylander-Clark, A. R. C., Hacker, B. R., and Craddock, J. P., 2017, The onset of the Dead Sea transform based on calcite age-strain analyses: Geology, v. 45(7), p. 587–590, doi:10.1130/G38903.1.

Parés, J.M., and van der Pluijm, B.A., 2002, Evaluating magnetic lineations (AMS) in deformed rocks: Tectonophysics, v. 350, p. 283–298.

Parés, J.M., and van der Pluijm,B.A., 2003, Magnetic fabrics and strain in pencil structures of the Knobs Formation, Valley and Ridge Province, US Appalachians: Journal of Structural Geology, v. 25, p.1349–1358.

Ron, H., Nowaczyk, N.R., Frank, U., Marco, S., and McWilliams, M.O., 2006, Magnetic properties of Lake Lisan and Holocene Dead Sea sediments and the fidelity of chemical and detrital remanent magnetization, in: Enzel, Y., Agnon, A. & Stein, M. (eds.), GSA book New Frontiers in Dead Sea Paleoenvironmental Research, GSA Special Paper 401, 171–182.

Schwehr, K., and Tauxe, L., 2003, Characterization of soft-sediment deformation: Detection of cryptoslumps using magnetic methods: Geology, v. 31, p. 203-206.

Tauxe, L., 1998, Paleomagnetic Principles and Practice: Kluwer Academic Publishers, Boston, Massachusetts. 299 p.

Weinberger, R., Levi, T., Alsop, G.I., and Eyal, Y., 2016, Coseismic horizontal slip revealed by sheared clastic dikes in the Dead Sea Basin: Geological Society of America Bulletin, v. 128(7/8), p. 1193–1206. doi:10.1130/B31415.1.

Weinberger, R., Levi, T., Alsop, G.I., and Marco, S., 2017, Kinematics of Mass Transport Deposits revealed by magnetic fabrics: Geophysical Research Letters, v. 44, p. 1-8, doi: 10.1002/2017GL074471.

FIGURE CAPTIONS

Figure 1. (a) General tectonic map showing the location of the study area (small red box) along the Dead Sea Fault (DSF) system. (b) Map of the Dead Sea Basin showing outcrops of the Lisan Formation and the position of strands of the DSF system. DSWBF - Dead Sea Western Border Fault zone. Fault trace at surface and fault trace based on subsurface data are marked by black and dashed lines, respectively.

Figure 2. (a) A normal fault from Masada Plain with a breccia layer located at the hanging wall on the right. (b) Two sets of slumps in Ami'az Plain cross cut by an injection clastic dike. (c) An injection clastic dike in Amia'z Plain filled with clay-rich sediment, cross-cutting the Lisan Formation about 12 m above its source layer.

Figure 3. A *T*- ln(*L*) plot. The grey and the dashed lines represent two possible types of correlation curves: (1) linear marked by "A" and and (2) nonlinear marked by "B" curve. Infilled white dot indicates an undefined value *T*=0. Solid black dot indicates *T*=-1 where k_2=k_3.

Figure 4. (a) A *T*-*L* plot of different seismite types containing aragonite material. Regions where the *T* and *L* values associated with sedimentation, damage zone, folding are marked schematically by a dashed purple line (polygon # A), dashed red line (polygon # B) and dashed dark line (polygon #C), respectively. The solid black line marks the linear correlation curve (y=-55x+1; R^2=0.95). (b) A *T*-*L* plot of different seismite types containing detrital material. Regions where the *T* and *L* values are associated with folding and injection are marked by a dashed dark line (polygon # D) and dashed green line (polygon # E), respectively. The black solid line marks the linear correlation curve of the folds (y==-84x+1; R^2=0.96) and the green solid and dashed lines mark the nonlinear correlation curves of the vertical (y==-0.4lnx-2; R^2=0.68) and the horizontal (y=-0.3lnx-1.4; R^2=0.94) injections, respectively.

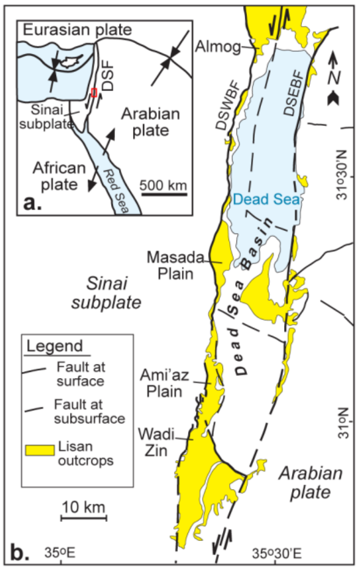
Eurasian plate
DSF
Sinai subplate
Arabian plate
African plate
Red Sea
500 km
a.
Almog
DSWBF
DSEBF
N
31o30'N
Dead Sea
Masada Plain
Dead Sea Basin
Sinai subplate
Legend
Fault at surface
Fault at subsurface
Lisan outcrops
Ami'az Plain
Wadi Zin
31oN
Arabian plate
10 km
b.
35oE
35o30'E

Figure 1

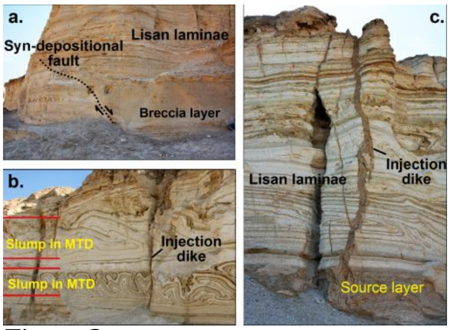
a.
Syn-depositional fault
Lisan laminae
Breccia layer
b.
Slump in MTD
Slump in MTD
Injection dike
c.
Lisan laminae
Injection dike
Source layer
Figure 2

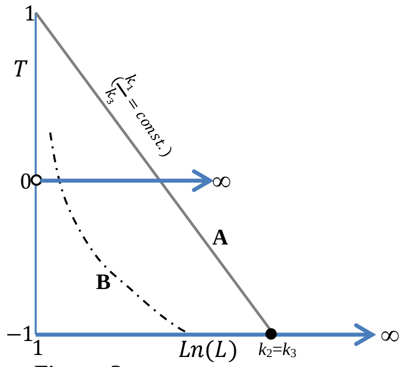

Figure 3

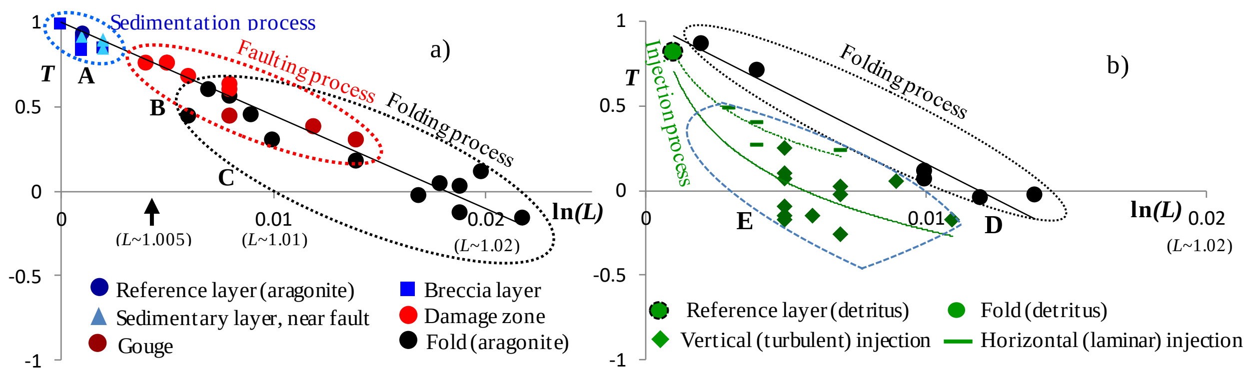

Sedimentation process
Faulting process
Folding process
a)
T
A
B
C
1
0.5
0
-0.5
-1
0
0.01
0.02
ln(L)
(L~1.005)
(L~1.01)
(L~1.02)
Reference layer (aragonite)
Sedimentary layer, near fault
Gouge
Breccia layer
Damage zone
Fold (aragonite)
b)
Folding process
Injection process
E
D
Reference layer (detritus)
Fold (detritus)
Vertical (turbulent) injection
Horizontal (laminar) injection

Figure 4